International Journal of Mining Science and Technology 28 (2018) 849–857

Contents lists available at ScienceDirect

International Journal of Mining Science and Technology

journal homepage: www.elsevier.com/locate/ijmst

Groundwater monitoring of an open-pit limestone quarry: Water-rock interaction and mixing estimation within the rock layers by geochemical and statistical analyses

Khy Eam Eang [a,*], Toshifumi Igarashi [b], Megumi Kondo [c], Tsurugi Nakatani [d], Carlito Baltazar Tabelin [e], Ryota Fujinaga [a]

[a] Laboratory of Groundwater and Mass Transport, Division of Sustainable Resources Engineering, Graduate School of Engineering, Hokkaido University, Sapporo 060-8628, Japan
[b] Laboratory of Groundwater and Mass Transport, Division of Sustainable Resources Engineering, Faculty of Engineering, Hokkaido University, Sapporo 060-8628, Japan
[c] Mitsubishi Materials Corporation, Tokyo 1008117, Japan
[d] Ryoko Lime Industry Co., Ltd., Chichibu-gun, Saitama 3680072, Japan
[e] Laboratory of Mineral Processing and Resources Recycling, Division of Sustainable Resources Engineering, Faculty of Engineering, Hokkaido University, Sapporo 0608628, Japan

ARTICLE INFO

Article history:
Received 27 October 2017
Received in revised form 1 February 2018
Accepted 10 April 2018
Available online 16 April 2018

Keywords:
Water-rock interaction
Groundwater mixing
Interbedded layer
Geochemist's workbench
Rock slope stability

ABSTRACT

Water-rock interaction and groundwater mixing are important phenomena in understanding hydrogeological systems and the stability of rock slopes especially those consisting largely of moderately water-soluble minerals like calcite. In this study, the hydrogeological and geochemical evolutions of groundwater in a limestone quarry composed of three strata: limestone layer (covering), interbedded layer under the covering layer, and slaty greenstone layer (basement) were investigated. Water-rock interaction in the open-pit limestone quarry was evaluated using PHREEQC, while hierarchical cluster analysis (HCA) and principal component analysis (PCA) were used to classify and identify water sources responsible for possible groundwater mixing within rock layers. In addition, Geochemist's Workbench was applied to estimate the mixing fractions to clarify sensitive zones that may affect rock slope stability. The results showed that the changes in Ca^{2+} and HCO_3^- concentrations of several groundwater samples along the interbedded layer could be attributed to mixing groundwater from the limestone layer and that from slaty greenstone layer. Based on the HCA and PCA results, groundwaters were classified into several types depending on their origin: (1) groundwater from the limestone layer (L_O), (2) mixed groundwater flowing along the interbedded layer (*e.g.*, groundwater samples L-7, L-11, S-3 and S-4), and (3) groundwater originating from the slaty greenstone layer (S_O). The mixing fractions of 41% L_O: 59% S_O, 64% L_O: 36% S_O, 43% L_O: 57% S_O and 25% L_O: 75% S_O on the normal days corresponded to groundwaters L-7, L-11, S-3 and S-4, respectively, while the mixing fractions of groundwaters L-7 and L-11 (61% L_O: 39% S_O and 93% L_O: 7% S_O, respectively) on rainy days became the majority of groundwater originating from the limestone layer. These indicate that groundwater along the interbedded layer significantly affected the stability of rock slopes by enlarging multi-breaking zones in the layer through calcite dissolution and inducing high water pressure, tension cracks and potential sliding plane along this layer particularly during intense rainfall episodes.

1. Introduction

In limestone quarries, groundwater chemistry is mainly dominated by the dissolution of calcite, the major mineral component of limestones, because it is moderately soluble in water [1]. The density, permeability and porosity of limestones primarily depend on the degree of consolidation and development of permeable zones after deposition. Prolonged dissolution may result in enlargement of pore space, which ultimately leads to the development of karst terrain, sinkholes, caves or various features, indicating that the effects of carbonate dissolution on water compositions are quite conspicuous. Consequently, understanding water-rock interaction is critical in evaluating changes in chemical compositions of groundwater along flow paths [2]. Domenico [3] and

* Corresponding author.
E-mail addresses: khyeam_eang@yahoo.com (K.E. Eang), tosifumi@eng.hokudai.ac.jp (T. Igarashi), mkondo@mmc.co.jp (M. Kondo), t-nakatani@ryokolime.co.jp (T. Nakatani), carlito@eng.hokudai.ac.jp (C.B. Tabelin), fujinaga@trans-er.eng.hokudai.ac.jp (R. Fujinaga).

https://doi.org/10.1016/j.ijmst.2018.04.002
2095-2686/

Toth [4] also note that groundwater evolves chemically by interacting with aquifer minerals and internal mixing among different groundwaters along flow paths. Moreover, variations of groundwater properties may help distinguish groundwater sources and aid in the identification of different geological formations.

The chemical composition of a newly formed groundwater is initially dependent on rainwater [5]. As rainwater percolates through soil or sediments, the chemical composition changes, especially when fairly soluble carbonate minerals like calcite and dolomite exist in the flow path. For example, the saturation index with respect to calcite is one of the important parameters used to evaluate groundwater flow in many limestone aquifer systems [6]. Because there are many variables involved in the evolution of groundwater, multivariate statistical analyses, in particular the hierarchical cluster analysis (HCA) and principal component analysis (PCA), are often employed to classify, interpret and quantify data on groundwater geochemistry. Love et al. [7], for example, applied PCA to distinguish signatures of uncontaminated groundwater with those impacted by agricultural activities, mining activities and sewage pollution. Similarly, Farnham et al. [8] and Mahlknecht et al. [9] used PCA to discuss geochemical evolution, mineralization and groundwater contamination in the Ash Meadows-Death Valley of Nevada and central Mexico, USA, respectively. The HCA has also been used to interpret hydrochemical data based on factor scores by Kim et al. [10] and Reghunath et al. [11].

Existence of groundwater in mine sites potentially causes slope stability problems [12]. In Japan, for example, there have been several rock slope failures in the limestone quarries partly attributed to groundwater [13]. In recent years, the flow and potentiometric level of groundwater are two of the most important factors affecting the stability of rock slopes [14,15]. In the study area, Kondo et al. [16] and Ozawa et al. [17] revealed that the rock slope was observed to be deformed in response to elevated groundwater levels after intense rainfall events, so groundwater in each geological formation has been monitored and often extracted to lower groundwater levels. Their monitored results of crack growths, however, revealed that lowering groundwater at some levels was somehow insufficient to prevent the continued deformation of rock slopes because other factors that were not considered in these previous studies also affect slope stability. One important parameter related to the instability is the dramatic change in water-rock interaction due to variations in groundwater flow and groundwater mixing in flow paths within the three rock strata. Unfortunately, there are very few papers that examine the stability of rock slope in limestone quarries from the point of view of geochemistry.

The objectives of this study are to elucidate the contributions of water-rock interaction to slope stability in a limestone quarry, to classify groundwater samples and their sources, and finally, to estimate possible mixing of groundwaters between rock layers and predict possible sensitive zones affecting rock slopes by using geochemical models and statistical analyses.

2. Materials and methods

2.1. Site description

The open-pit limestone quarry in this study is located in the mountainous region of Chichibu city in Saitama prefecture, Japan (Fig. 1). The quarry mainly consists of three rock strata: (1) limestone as a covering rock layer, (2) an interbedded layer of limestone and slaty greenstone underlying the covering rock, and (3) slaty greenstone as basement rock (Fig. 2a). In the covering layer, limestone is mostly grayish to white, microcrystalline and compact. The limestone deposit in this area was formed in the Triassic

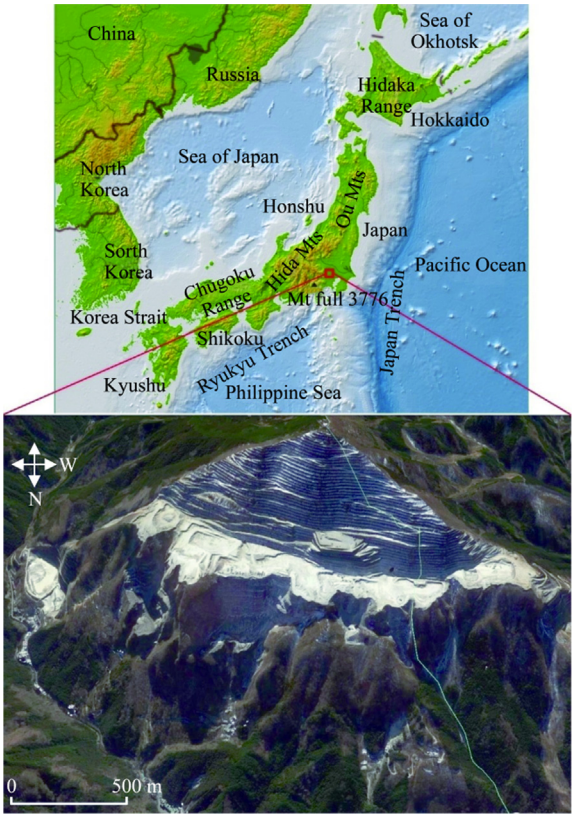

Fig. 1. Location of the limestone open-pit quarry in Chichibu city, Saitama.

period [18], covering the northern half of the mountain, extending 5 km east-westward with thicknesses between 500 and 700 m, and lies with a strike of N70°E and dip of 45°–80° north. In the interbedded layer, limestone and slaty greenstone are either interbedded or sometimes mixed in thicknesses of several centimeters to several meters. Limestone and slaty greenstone are both cryptocrystalline while the interbedded layer is characterized by multi-breaking zones. In the basement layer, slaty greenstone has a dark green to red purple color and was formed by alteration of basaltic rocks. Even though the basement slaty greenstone is solid, portions of it immediately below the interbedded layer have cracks, joints and weak faces because of structural movements and groundwater flow [19].

2.2. Sample collection and analysis procedure

To survey the geological and hydrological conditions inside the quarry, some underground tunnels were excavated. Several boreholes in each tunnel were also drilled upward to drain and monitor groundwater levels. The cross sectional and plan views of the limestone quarry with sampling points are illustrated in Fig. 2a and b. Eleven groundwater sampling campaigns were conducted from December 2014 to November 2016. Thirteen groundwater samples in the limestone layer (L-1–L-11, LP-1 and LP-10) and four in the slaty greenstone layer (S-1–S-4) were collected in each sampling campaign. In total, 160 groundwater samples (121 from the limestone layer and 39 from the slaty greenstone layer) were collected in and around the study area.

Geochemical properties of groundwater were monitored and analyzed periodically. Temperature, pH, oxidation-reduction potential (ORP) and electrical conductivity (EC) of groundwater samples were measured in situ. Their flow rates were also measured by the volumetric method. The groundwater samples were divided into two parts on site in preparation for the chemical

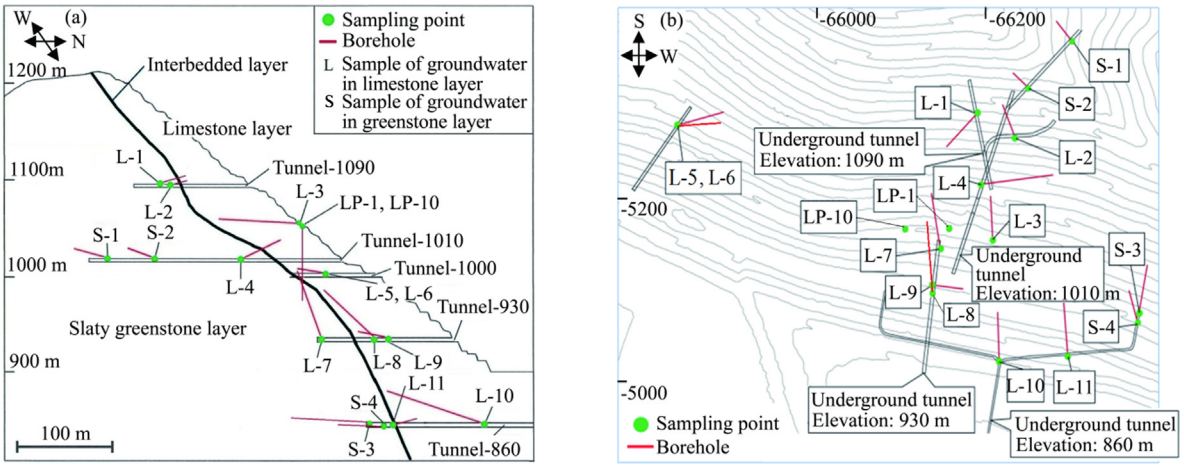

Fig. 2. Cross sectional view of the limestone quarry (a) and plan view of sampling points of groundwater (b).

analyses. The first one was unfiltered and stored in 250 mL bottles with no air bubble, tightly capping and sealing with plastic tape to avoid degassing or air contact while the second one was filtered through 0.45 μm Millex® membrane filters (Merck Millipore, USA) and stored in 100 mL bottles. The alkalinity was measured by titration with 0.01 M sulfuric acid in the laboratory immediately after receiving the samples from the quarry. Concentrations of dissolved ions and trace elements were measured using ion chromatographs (ICS-90 and ICS-1000, Dionex Corporation, USA) and an inductively-coupled plasma atomic emission spectrometer (ICP-AES, ICPE-9000, Shimadzu Corporation, Japan), respectively. Ion chromatographs and ICP-AES both have margins of error about 2–3%.

2.3. Water-rock interaction

The geochemical evolution of groundwater in the study area is mainly related to changes of Ca^{2+} and HCO_3^- concentrations due to calcite dissolution ($CaCO_3+CO_{2(g)}+H_2O \rightleftharpoons Ca^{2+}+2HCO_3^-$) as reported in the previous studies by Eang et al. [20], so the relationship between these two ions was closely monitored. The calculated saturation indices of calcite ($SI_{calcite}$) by PHREEQC were used to understand water-rock interaction and possible mixing of groundwater in the flow paths.

2.4. Multivariate statistical analysis

In hydrogeochemical studies, multivariate statistical analysis is a quantitative and independent approach of groundwater classification (such as grouping groundwater samples and making correlations among the chemical parameters and the samples) and groundwater source identification [21]. In this paper, two multivariate methods, HCA and PCA, were applied using OriginLab (OriginLab Corp., USA) with the representative dataset of 17 samples from December 2014 to November 2016. The representative dataset here referred to the dataset of each sample from eleven groundwater sampling campaigns by mixing with equal proportion in volume (*e.g.*, L-1 from eleven time collections were mixed altogether with equal proportion in volume by Smart Mix function of Geochemist's Workbench to produce the representative L-1 and the same methods for other samples). This representative dataset roughly accounted for the average values, but they may shift a little from the average ones due to the effect of various pH values. By doing so, the dataset became more appropriate especially aiming for mixing of groundwater collected from different periods.

HCA is a data classification technique. Although there are various clustering techniques, HCA is one of the most common methods in earth science and often applied in the classification of hydrogeochemical data [22,23]. In this study, HCA was carried out with 8 parameters (Na^+, Mg^{2+}, K^+, Ca^{2+}, Cl^-, SO_4^{2-}, NO_3^- and HCO_3^-) and the Euclidean distance was utilized as the distance measure or similarity measurement between sampling sites. The sampling sites with the greater similarity are grouped first, and then the steps are repeated until all observations have been classified. Finally, samples were grouped and assigned into the specific clusters under the fixed phenon line. To avoid misclassifications arising from the different orders of magnitude of variables or from the effect of parameters with the highest variances on the calculation of Euclidean distance [24,25], the variance of each variable was standardized as reported by Davis and Sampson [26], and meq/L unit was used to categorize different behaviors of groundwater in the rock layers.

PCA is a data transformation technique and also one of the most widely used multivariate statistical methods in natural sciences, which was developed by Hotelling [27] from the original work of Pearson. The principal components were computed using the standardized data. The general objective of this technique is to simplify data structure by reducing dimension of the data. In this paper, PCA was applied with 11 parameters of temperature, pH, EC and eight ions. The original parameters would be rearranged into several new uncorrelated comprehensive components (or factors) without losing significant information [28,29]. The calculated components were rotated with the Varimax rotation method, thus creating the loadings of closely related variables in each strengthened component. By the orthogonal projection of the variables on each of the components, the variable loadings were determined. The selected components were based on both the significance (Eigenvalue >1) of the component and the cumulative percentage of explained variance. Finally, the significant step was to interpret each factor in association with the studied issue; however, the main target of this application was aimed to distinguish groundwater samples and to propose the mixing model.

2.5. Groundwater mixing estimation using Flash Diagram

By considering the geochemical data and the results of HCA and PCA, the conceptual model of groundwater mixing was constructed. Using the Flash Diagram function in Geochemist's Workbench® version 11 (GWB, Aqueous Solution LLC), mixing fractions of the groundwater formed by mixing between two different groundwaters were estimated. Most of the geochemical data (*e.g.*, pH, temperature, concentrations of Ca^{2+}, HCO_3^-, Na^+, Mg^{2+}, K^+, Cl^-, SO_4^{2-}, NO_3^- and Si) were employed as the input parameters. In this

study, the concentrations of Ca^{2+} and HCO_3^- were key indicators because calcite dissolution within groundwater flow paths played an important role, whereas the concentrations of other ions were very low, almost constant and apparently independent of the geological formation of the study area. Mixing fractions versus Ca^{2+} concentrations were considered in the plot from Flash Diagram (see more descriptions in Section 3.5). The mixing fractions of mixed groundwater were derived from the plot relying on the Ca^{2+} concentrations. Based on groundwater flow paths and mixing conditions, sensitive zones affecting the stability of rock slopes were ultimately identified.

3. Results and discussion

3.1. Preliminary results of rock properties

The mineral and chemical compositions of representative rock samples such limestones in the covering and interbedded layers, and slaty greenstones in the interbedded and basement layers were analyzed by X-ray powder diffraction (XRD) and X-ray fluorescence (XRF), respectively. From the XRD results, limestones in the covering and interbedded layers consist of calcite as their major mineral component. Slaty greenstone in the interbedded layer consists of quartz, albite, calcite, chlorite and hematite while that in the basement layer consists of quartz, albite, chlorite and hematite. From the XRF results, limestones in the covering and interbedded layers contain substantial amounts of CaO with 54.6% and 52.9% (by weight), respectively. Meanwhile, the slaty greenstones contain 38.5% to 39.7% (by weight) of SiO_2 as the main chemical component. Details of the chemical and mineralogical composition of the different strata have been previously described by Eang et al. [20].

3.2. In situ measurements of groundwater

The results of in situ measurements of groundwater are presented in Fig. 3. The flow rates of groundwater in the covering layer ranged from 0.01 to 298 L/min and had larger fluctuations than that of the basement rock ranging from 0.02 to 69.9 L/min (Fig. 3a) because the hydraulic conductivity of the former (4.1×10^{-6} m/s) was about two orders of magnitude higher than that of the latter (4.2×10^{-8} m/s) (Note: samples LP-1, LP-10 and S-3 were not included in the figure because they were pumped periodically or the flow rates were not measurable). In Fig. 3b, temperatures of groundwater ranged from 6 to 17.9 °C in the limestone layer and were somewhat higher than those in the slaty greenstone layer (8.8–10.5 °C). In Fig. 3c, pH values of groundwater in the limestone layer ranged from 7.7 to 8.4 and were lower than those of groundwater in the slaty greenstone layer (7.8–8.6), which could be attributed to higher partial pressure of $CO_{2(g)}$ in the limestone layer [20]. In Fig. 3d, EC values of groundwater in the limestone layer ranged from 15.9 to 26.5 mS/m and were higher than those of groundwater in the slaty greenstone layer (11.1–16.9 mS/m), suggesting that higher total dissolved solids in the limestone layer were because of the dissolution of calcite. In Fig. 3e, ORP values of groundwater ranged from 0.075 to 0.25 V in the limestone layer and from 0.10 to 0.21 V in the slaty greenstone layer, indicating that there were no significant differences between the two layers. Also, the groundwater samples were under oxidizing conditions (ORP > 0).

3.3. Water rock-interaction

The relationship between Ca^{2+} and HCO_3^- concentrations is illustrated in Fig. 4. The concentrations in meq/L were used in this paper. The Ca^{2+} and HCO_3^- concentrations of groundwater in the limestone layer were generally higher than those in the slaty greenstone layer. This is to be expected because the limestone has higher calcite content than the slaty greenstone. In addition, the Ca^{2+} and HCO_3^- concentrations of samples L-7 and L-11 were relatively lower than the other samples from the limestone layer, whereas the Ca^{2+} and HCO_3^- concentrations of samples S-3 and S-4 were fairly higher than those of samples S-1 and S-2 in the slaty greenstone layer. Therefore, groundwaters from L-7, L-11, S-3 and S-4 may have originated from the mixing of groundwaters from the limestone and slaty greenstone layers because these sampling

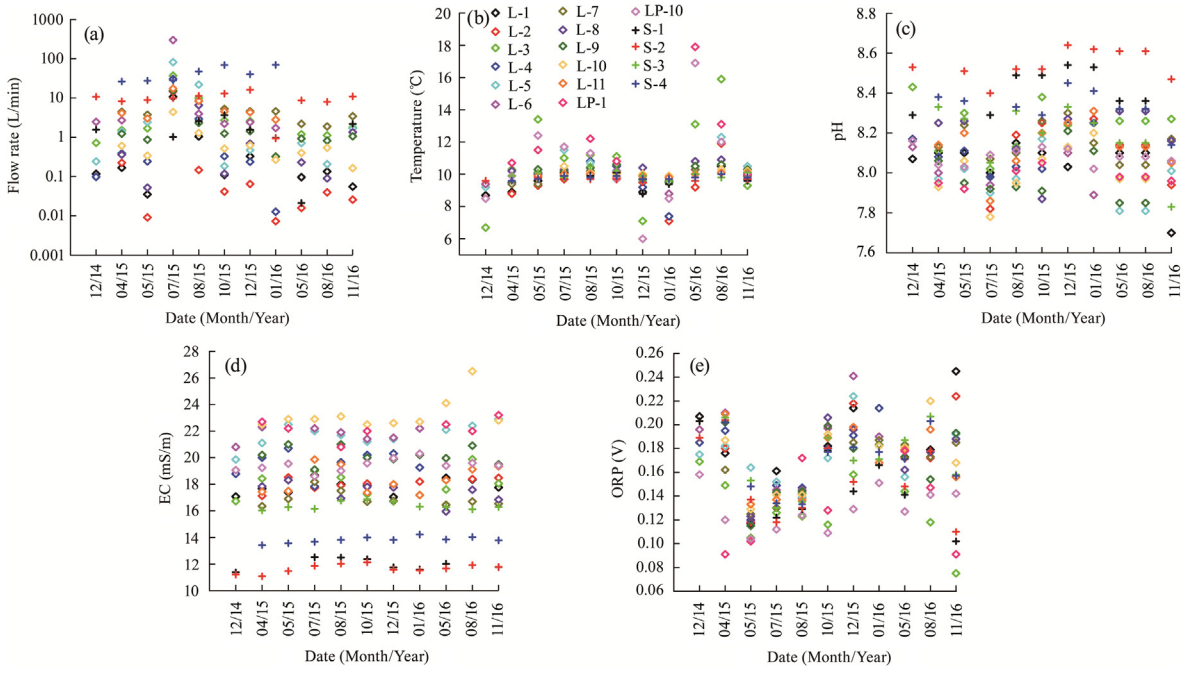

Fig. 3. Flow rate (a), temperature (b), pH (c), EC (d) and ORP (e) of all groundwater samples collected from December 2014 to November 2016.

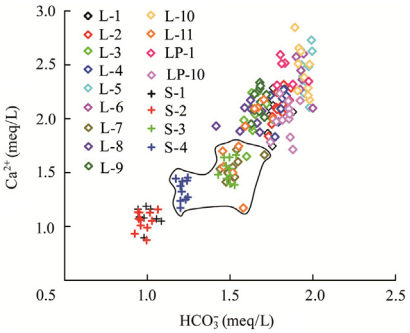

Fig. 4. Relationship between Ca^{2+} and HCO_3^- concentrations of all groundwater samples (⌓: circled area indicates the groundwater samples that may have originated from mixing of groundwaters from the limestone and slaty greenstone layers).

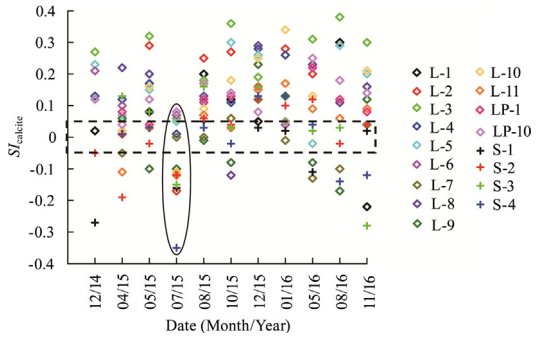

Fig. 5. $SI_{calcite}$ of all groundwater samples (⌐¬: dashed rectangle indicates the saturated condition of calcite mineral; ⌓: circled area indicates the rainy days).

points were located near the interbedded layer, which is the boundary layer.

The distribution of $SI_{calcite}$ of groundwater samples is plotted in Fig. 5. The $SI_{calcite}$ of groundwater in the limestone layer was mostly larger than zero and also greater than the $SI_{calcite}$ of groundwater in the slaty greenstone layer. The $SI_{calcite}$ decreased in July 2015, which suggests that the recharge of rainwater corresponds to young groundwater in term of residence time [30]. This means that the groundwater mixed with rainwater may not have sufficient time to equilibrate with calcite owing to the faster flow rate. Merkel and Planer-Friedrich pointed out that a *SI* range of 0 ± 0.05 was supposed to be in equilibrium due to inherent uncertainties in calculation of *SIs* such as the accuracy of chemical analysis, mineral equilibrium constant and the method of calculating ion activities [31]. This means that most of the groundwater samples from the limestone layer were supersaturated or in equilibrium with calcite except those collected in July 2015. The groundwater samples in the slaty greenstone layer were dominantly in equilibrium or undersaturated with calcite. From Batoit et al. [32] and Wigley and Plummer [33], mixing of two groundwaters with different compositions can lead to undersaturation of calcite in the resulting groundwater leading to the renewed dissolution of calcite in carbonate aquifers, even if the two original groundwaters are in equilibrium before mixing. Also, the general compositions of mixed groundwater would lie somewhere between the compositions of the original groundwaters. Therefore, the change in quality of groundwater samples L-7, L-11, S-3 and S-4 was most likely caused by mixing groundwater from the limestone covering layer and slaty greenstone basement layer. On the rainy days, the mixing was also affected by rainwater infiltrating through the limestone covering layer.

3.4. Multivariate statistical analysis

3.4.1. Hierarchical cluster analysis

As part of HCA results, the descriptive statistics are given in Table 1 to summarize the characteristics and variation between clustering variables, whereas the procedure of cluster stages, statistically grouping from the smallest to the highest distances, is presented in Table 2.

To quantify the similarity of the samples, HCA was then performed based on the concentrations of major ions in groundwater, and the dendrogram of HCA is presented in Fig. 6. The phenon line determined the number of clusters by mainly considering the significant variation of Ca^{2+}–HCO_3^- distributions. As a result, the phenon line was defined as the distance of 0.6, by which all samples were classified into three statistically significant clusters (which represented the similarity of the individual samples). Cluster I was composed of the groundwater samples mainly located in the limestone layer with larger similarity (*e.g.*, higher concentrations of Ca^{2+} and HCO_3^-) and stable quality. These groundwaters were regarded as an original groundwater from the covering layer. Most samples in Cluster II were located along the interbedded layer, where the groundwaters were possibly mixed between groundwaters from the limestone and slaty greenstone layers (and/or infiltrated rainwater during the rainy days). However, groundwater sample S-4 was not in this cluster because it was not dramatically mixed with groundwater from the limestone layer. Cluster III basically consisted of groundwaters from the basement slaty greenstone layer. Groundwaters from S-1 and S-2 had similar and stable quality, for example, lower concentrations of Ca^{2+} and HCO_3^-. In consequence, these two groundwaters were assumed to be the original groundwater from the basement slaty greenstone layer.

3.4.2. Principal component analysis

As part of PCA results, the symmetrical correlation matrix was computed as shown in Table 3. The result shows that EC, Ca^{2+} and HCO_3^- were in positively high correlations with each other (with correlation coefficients >0.9) due to calcite dissolution and

Table 1
Descriptive statistics of the concentrations (meq/L) of eight ions.

Parameters	*N*	Mean	*SD*	Sum	Min	Median	Max
Na^+	17	0.067	0.026	1.147	0.031	0.075	0.119
Mg^{2+}	17	0.131	0.094	2.235	0.031	0.087	0.310
K^+	17	0.006	0.002	0.109	0.003	0.006	0.011
Ca^{2+}	17	1.911	0.454	32.49	1.048	2.021	2.446
Cl^-	17	0.029	0.007	0.489	0.019	0.028	0.050
SO_4^{2-}	17	0.184	0.100	3.120	0.068	0.169	0.382
NO_3^-	17	0.037	0.032	0.631	0.013	0.021	0.097
HCO_3^-	17	1.653	0.320	28.10	0.978	1.720	2.003

Note: *SD*: standard deviation and *N*: number of representative samples.

Table 2
Cluster stages of statistical grouping.

Stage	Distance	Cluster 1	Cluster 2	Number of clusters	New cluster	Next stage
1	0.045	14	15	16	14	13
2	0.048	3	8	15	3	9
3	0.056	5	6	14	5	8
4	0.057	1	2	13	1	7
5	0.127	10	12	12	10	8
6	0.133	7	16	11	7	12
7	0.145	1	4	10	1	9
8	0.170	5	10	9	5	14
9	0.202	1	3	8	1	10
10	0.230	1	13	7	1	11
11	0.239	1	9	6	1	14
12	0.330	7	11	5	7	15
13	0.360	14	17	4	14	15
14	0.457	1	5	3	1	16
15	0.692	7	14	2	7	16
16	1.004	1	7	1	1	

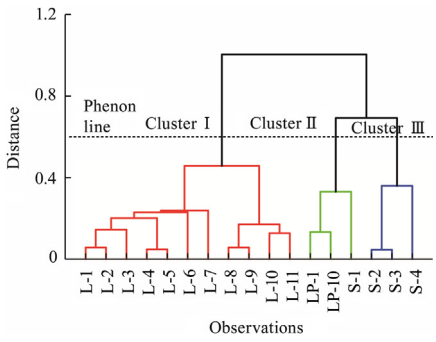

Fig. 6. Dendrogram from the HCA for all groundwater samples.

next followed by Mg^{2+} and Na^{+} (with a correlation coefficient of 0.86), which may result from the dissolved ionic compounds of Mg and Na-bearing minerals. On the other hand, EC, Ca^{2+} and HCO_3^- were in negatively strong correlations with pH (with correlation coefficients <−0.9), simply explained that the solubility of $CaCO_3$ increased with a decrease in pH (*e.g.*, the lower pH induced the higher dissolution of $CaCO_3$).

The rotated factor loadings of principal components on variables and the biplot from PCA are illustrated in Table 4 and Fig. 7, respectively. Three major principal components (PC1, PC2, and PC3) affecting the quality of groundwater are identified, which accounted for 85.4% as the cumulative variance of the original data structure (Table 4). The data shown in bold in Table 4 indicate the relatively significant loading and contribution to the responding components. PC1, which explained 53.6% of the total variance, had strong loadings on pH, EC, Ca^{2+}, NO_3^- and HCO_3^-. The pH and NO_3^- both had the negative coefficients to this factor and they were positively correlated with each other, whereas the EC and the major ions (Ca^{2+} and HCO_3^-) had the positive coefficients governed by water-rock interaction in the flow path. PC2 accounted for 19.2% of the total variance, which was positively correlated with Na^{+}, Mg^{2+}, K^{+} and SO_4^{2-}, representing the major ions except Ca^{2+} and HCO_3^- and probably indicating the impact of Na, Mg and K-bearing minerals in association with SO_4 into groundwater as well. Lastly, 12.6% of the total variance was explained by PC3. Temperature and Cl^- contributed to PC3. Since PC1 and PC2 governed the majority of the loadings, PC1 and PC2 were considered in the biplot (combination of loadings and scores) from PCA (Fig. 7). The plots show the characteristics of the components and help to clearly understand the relative importance of variables in components. Essentially, the samples in Cluster I were plotted along the positive side of PC1, indicating that their geochemistry was mainly controlled by calcite dissolution. These samples statistically corresponded to the original groundwater in the covering limestone layer. The samples in Cluster II were plotted in negative and positive directions of PC1 and PC2, respectively, and interpreted as the mixed groundwater between the groundwater from the limestone layer and groundwater from the slaty greenstone layer, and/or rainwater infiltrating through the limestone layer. The samples in Cluster III were plotted in negative directions of PC1 and PC2. However, groundwater sample S-4 was slightly shifted to the upper zone close to Cluster II, indicating that this groundwater was somewhat mixed between the groundwater from the covering limestone and basement slaty greenstone layers, while groundwaters from S-1 and S-2 statistically regarded as the original groundwater in the basement layer.

Table 3
Correlation matrix of temperature (°C), pH, EC (mS/m) and concentrations (meq/L) of eight ions.

Parameters	Temp.	pH	EC	Na^{+}	Mg^{2+}	K^{+}	Ca^{2+}	Cl^-	SO_4^{2-}	NO_3^-	HCO_3^-
Temp.	1.000										
pH	−0.346	1.000									
EC	0.447	**−0.944**	1.000								
Na^{+}	0.075	0.182	−0.256	1.000							
Mg^{2+}	−0.200	0.511	−0.589	**0.863**	1.000						
K^{+}	0.080	−0.058	−0.020	0.546	0.467	1.000					
Ca^{2+}	0.409	**−0.902**	**0.971**	−0.460	−0.758	−0.156	1.000				
Cl^-	0.203	0.370	−0.242	0.043	0.027	−0.158	−0.205	1.000			
SO_4^{2-}	0.547	−0.702	0.771	0.179	−0.223	0.011	0.667	−0.054	1.000		
NO_3^-	−0.278	0.754	−0.762	0.457	0.640	−0.118	−0.789	0.320	−0.400	1.00	
HCO_3^-	0.324	**−0.926**	**0.966**	−0.391	−0.635	−0.015	**0.964**	−0.345	0.596	−0.83	1

Notes: Values in bold numbers indicate very significant correlations; Temp.: temperature.

Table 4
Rotated factor loadings of principal components on variables.

Parameters	Coefficients of PC1	Coefficients of PC2	Coefficients of PC3
Temp.	0.178	0.246	**0.529**
pH	**−0.380**	−0.164	0.104
EC	**0.399**	0.125	0.034
Na^+	−0.184	**0.587**	0.057
Mg^{2+}	−0.305	**0.418**	−0.085
K^+	−0.045	**0.507**	−0.283
Ca^{2+}	**0.407**	−0.026	0.046
Cl^-	−0.114	−0.095	**0.690**
SO_4^{2-}	0.278	**0.332**	0.291
NO_3^-	**−0.349**	0.014	0.202
HCO_3^-	**0.398**	0.039	−0.118
Eigenvalue	5.90	2.11	1.38
Explained variance	53.63%	19.19%	12.56%
Cumulative	53.63%	72.82%	85.38%

Note: Values in bold numbers indicate the relatively significant loading and contribution to the responding components.

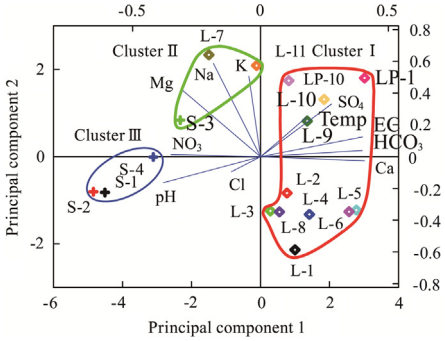

Fig. 7. Biplot from the PCA for all groundwater samples.

3.5. Groundwater mixing estimation using Flash Diagram

Based on all the above results and/or the previous findings suggested by Eang et al. [20], conceptual models of mixing are constructed into two cases as follows:

(1) Case of normal days–all sampling periods except July 2015 (Fig. 8a and b):

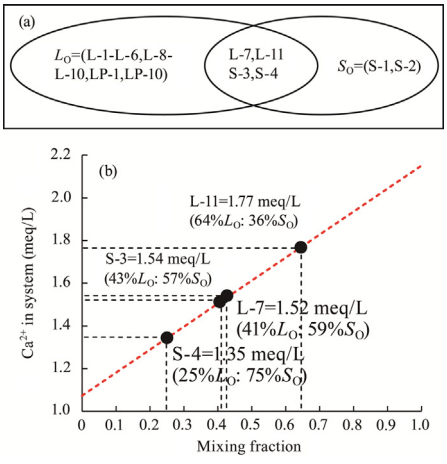

Fig. 8. Conceptual model of groundwater mixing for normal days (L_O and S_O: original groundwater from the limestone and slaty greenstone layers, respectively) (a) and results of mixing estimation using Flash Diagram for the normal days (b).

Conceptual model of groundwater mixing for the case of normal days is presented in Fig. 8a. Groundwaters from L-7, L-11, S-3 and S-4 were assumed to be mixtures of original groundwater from the limestone (L_O) and slaty greenstone layers (S_O). Note that every sample was in general from ten time collections for the case of normal days (*i.e.*, all sampling periods except July 2015). Thus, the representative of individual samples was basically carried out in the concept of mixing (*e.g.*, L-1 samples from ten time collections were mixed together with an equal proportion in volume by GWB's Smart Mix function to produce the representative L-1 and the same methods for other samples, see the detailed explanation in Section 2.4). L_O was obtained by mixing equal proportions in terms of volume of samples L-1–L-6, L-8–L-10, LP-1 and LP-10 (by GWB's Smart Mix function) on the normal days, while S_O was obtained by mixing equal proportions in volume of samples S-1 and S-2, following the same method as L_O in this case.

Results of mixing estimation using Flash Diagram for the case of normal days are shown in Fig. 8b. The red-dashed line represents the mixing fraction results (after the original groundwater from the limestone layer (L_O) was flashed into the original groundwater from the slaty greenstone layer (S_O)), whereas the lowest end of red-dashed line indicates Ca^{2+} concentration of S_O and its top end indicates Ca^{2+} concentration of L_O. Based on Ca^{2+} concentrations, the mixing fractions of 41% L_O: 59% S_O and 64% L_O: 36% S_O corresponded to the representative Ca^{2+} concentration of L-7 and L-11, respectively, whereas the mixing fractions of 43% L_O: 57% S_O and 25% L_O: 75% S_O corresponded to the representative Ca^{2+} concentration of S-3 and S-4, respectively.

(2) Case of rainy days–sampling period on July 2015 (Fig. 9a and b):

Conceptual model of groundwater mixing for the case of rainy days is provided in Fig. 9a. Groundwaters from L-7, L-11, S-3 and S-4 were the mixture of original groundwaters from the limestone (L_O) and slaty greenstone layers (S_O) that were affected by rainwater (RW). L_O was obtained by mixing with equal proportions in volume of samples L-1–L-6, L-8–L-10, LP-1 and LP-10 (by GWB's Smart Mix function) on the rainy days, while S_O was obtained by mixing equal proportions in volume of samples S-1 and S-2, following the same method as L_O for the rainy days.

Results of mixing estimation using Flash Diagram for the case of rainy days are illustrated in Fig. 9b. Based on Ca^{2+} concentrations, the mixing fractions of 61% L_O: 39% S_O and 93% L_O: 7% S_O corresponded to the Ca^{2+} concentration of L-7 and L-11 on the rainy day, respectively, whereas the mixing fractions of 35% L_O: 65% S_O and 21% L_O: 79% S_O corresponded to the Ca^{2+} concentration of S-3 and S-4, respectively. These indicate that the mixing fractions of groundwater in the limestone layer in L-7 and L-11 were greater than those of S-3 and S-4 during rainy days, while the mixing fractions of S-3 and S-4 almost remained stable.

3.6. Overall evaluation of rock slopes

The mixing fractions of groundwater samples L-7 and L-11 significantly varied between normal and rainy days and the groundwater flowing through the limestone layer became dominant on the rainy days, whereas the mixing fractions of groundwater samples S-3 and S-4 were almost stable. According to Fitts [34] and Whitaker and Smart [35], groundwater integrated in the multi-breaking zones of the interbedded layer erodes limestone by dissolution and widens those breaking zones notably on the rainy days while calcite is likely to dissolve more in the undersaturated condition. These phenomena induce gradual crack growths and higher groundwater levels during the intense rainfall. Based on Appelo and Postma [1], the dominant flow mode of groundwater in

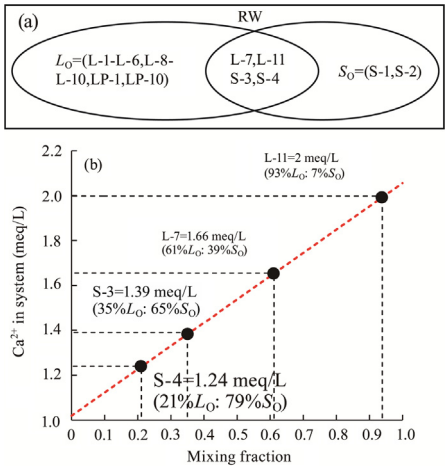

Fig. 9. Conceptual model of groundwater mixing for rainy days (L_O and S_O: original groundwater from the limestone and slaty greenstone layers, respectively; RW: rainwater) (a) and result of mixing estimation using Flash Diagram for the rainy days (b).

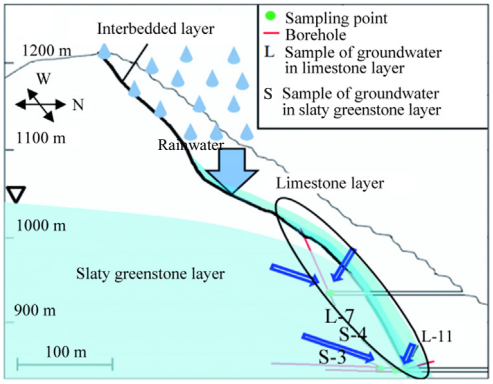

Fig. 10. Groundwater flow paths (⟹: blue arrows indicate L-7, L-11, S-3 and S-4 formed by groundwater mixing between the layers; ⬭: circled area indicates the sensitive zones).

this study is a conduit flow as suggested by the measured flow rates. It happens along larger fissures and openings formed from dissolution of carbonate rock. Apparently, changes in groundwater level and flow along the interbedded layer may promote pore-water pressure, tension cracks and potential sliding surface, which ultimately lead to a sliding failure along the interbedded layer. Due to the large differences in hydraulic conductivities between the two layers ($4.1 \times 10^{-6}/4.2 \times 10^{-8} \approx 100$, equal to the considerable ratio reported by Dong et al. [36]), groundwater mixed with rainwater may easily infiltrate and percolate through more permeable limestone covering layer but not through the slaty greenstone layer. In other words, the slaty greenstone layer with a lower permeability could act as a kind of groundwater barrier and lift the limestone covering layer up. The resultant higher hydraulic head in the limestone covering layer could increase groundwater flow and induce higher dissolution of limestone. The higher groundwater flow and more rapid dissolution of limestone grains will affect the bonds between particles and would often reduce the rock strength by more than 25% [37]. Regarding the various interpretations, the mixed groundwaters especially L-7 and L-11 along the interbedded layer were identified as sensitive zones affecting the stability of rock slope (Fig. 10).

4. Conclusions

By using the monitoring groundwater geochemistry from a limestone quarry and analyses of the data by PHREEQC, HCA, PCA and GWB, the findings of this study are summarized as follows:

(1) Water-rock interaction within the quarry was distinguished by individual layers, all of which were geochemically evolved as a function of calcite dissolution.
(2) The groundwater samples were classified into the original groundwater from the limestone layer, the mixed groundwater along the interbedded layer, and the original groundwater from the slaty greenstone layer. On rainy days, mixing fractions changed dramatically with the bulk of the mixture originating from groundwater flowing through the limestone layer.
(3) The groundwater along the interbedded layer may induce rock slope failure due to a higher mixed fraction in the interbedded layer.
(4) The above results suggest the necessity of continuous monitoring of groundwater.

Acknowledgments

The authors would like to deeply thank Ryoko Lime Industry Co., Ltd. for the permission to conduct research in the above study area, the kind support and the cooperation in every sampling campaign.

References

[1] Appelo CAJ, Postma D. Geochemistry, groundwater and pollution. London: A. A. Balkema Publishers; 2005.
[2] Belkhiri L, Mouni L, Tiri A. Water–rock interaction and geochemistry of groundwater from the Ain Azel aquifer. Algeria Environ Geochem Health 2012;34(1):1–13.
[3] Domenico PA. Concepts and models in groundwater hydrology. New York: McGraw-Hill; 1972.
[4] Toth J. The role of regional gravity flow in the chemical and thermal evolution of groundwater. In: Proceedings of the first Canadian/American conference on hydrogeology, Banff, Alta; 1984.
[5] Stumm W, Morgan JJ. Aquatic chemistry: an introduction emphasizing chemical equilibria in natural waters. New York: John Wiley & Sons, Inc.; 1981.
[6] Peyraube N, Lastennet R, Denis A, Malaurent P, Villanueva JD. Interpreting CO_2-SI_c relationship to estimate CO_2 baseline in limestone aquifers. Environ Earth Sci 2014;72:4207–15.
[7] Love D, Hallbauer D, Amos A, Hranova R. Factor analysis as a tool in groundwater quality management: two southern African case studies. Phys Chem Earth 2004;29(15–18):1135–43.
[8] Farnham IM, Johannesson KH, Singh AK, Hodge VF, Stetzenbach KJ. Factor analytical approaches for evaluating groundwater trace element chemistry data. Anal Chim Acta 2003;490(1–2):123–38.
[9] Mahlknecht J, Steinich B, Navarro de Léon I. Groundwater chemistry and mass transfers in the independence aquifer, central Mexico, by using multivariate statistics and mass-balance models. Environ Geol 2003;45(6):781–95.
[10] Kim JH, Kim RH, Lee J, Cheong TJ, Yum BW, Chang HW. Multivariate statistical analysis to identify the major factors governing groundwater quality in the coastal area of Kimje, South Korea. Hydrol Process 2005;19(6):1261–76.
[11] Reghunath R, Murthy TRS, Raghavan BR. The utility of multivariate statistical techniques in hydrogeochemical studies: an example from Karnataka, India. Water Res 2002;36(10):2437–42.
[12] Zhao L, Ren T, Wang N. Groundwater impact of open cut coal mine and an assessment methodology: a case study in NSW. Int J Min Sci Technol 2017;27(5):861–6.
[13] Yamaguchi U, Shimotani T. A case study of slope failure in a limestone quarry. Int J Rock Mech Min Sci Geomech Abstr 1986;23(1):95–104.
[14] Shen B, Poulsen B, Luo X, Qin J, Thiruvenkatachari R, Duan Y. Remediation and monitoring of abandoned mines. Int J Min Sci Technol 2017;27(5):803–11.
[15] Ulusay R, Ekmekci M, Tuncay E, Hasancebi N. Improvement of slope stability based on integrated geotechnical evaluations and hydrogeological conceptualisation at a lignite open pit. Eng Geol 2014;181:261–80.
[16] Kondo M, Nakatani K, Mikami K. Stabilization works for the final slope and procedures for validation of their effects in the Une limestone quarry. In: Proceedings of the Mining and Materials Processing Institute of Japan, Morioka; 2016, p. 1112.

[17] Ozawa K, Aoyama H, Kondo M, Nakatani K. Analysis on the final slope behaviors by rainfall and consideration on the effects of stabilizing measures. In: Proceedings of the Mining and Materials Processing Institute of Japan, Morioka; 2016, p. 1113.
[18] Hayashi S, Iijima S, Ishii I, Nakajima T, Sawaguchi H, Tanaka H. Late Paleozoic to Mesozoic formations in the southwestern Ashio Mountains. Bull Gunma Prefect Mus Hist 1990;11:1–34.
[19] Committee on the Long-Wall Rock Slope. Research on the stability of the long-wall rock slope of limestone quarries in Japan. Min Mater Process Inst Japan; 2013.
[20] Eang KE, Igarashi T, Fujinaga R, Kondo M, Tabelin CB. Groundwater monitoring of an open-pit limestone quarry: groundwater characteristics, evolution and their connections to rock slopes. Environ Monit Assess 2018;190(193):1–15.
[21] Cloutier V. Origin and geochemical evolution of groundwater in the Paleozoic Basses-Laurentides sedimentary rock aquifer system, St. Lawrence Lowlands, Québec, Canada. Québec, Canada: INRS-Eau, Terre & Environnement; 2004.
[22] Davis JC. Statistics and data analysis in geology. New York: John Wiley & Sons, Inc.; 1986.
[23] Güler C, Thyne GD, McCray JE, Turner KA. Evaluation of graphical and multivariate statistical methods for classification of water chemistry data. Hydrogeol J 2002;10(4):455–74.
[24] Cloutier V, Lefebvre R, Therrien R, Savard MM. Multivariate statistical analysis of geochemical data as indicative of the hydrogeochemical evolution of groundwater in a sedimentary rock aquifer system. J Hydrol 2008;353(3–4):294–313.
[25] Jiang Y, Guo H, Jia Y, Cao Y, Hu C. Principal component analysis and hierarchical cluster analyses of arsenic groundwater geochemistry in the Hetao basin, Inner Mongolia. Chem Erde 2015;75(2):197–205.
[26] Davis JC, Sampson RJ. Statistics and data analysis in geology. New York: Wiley; 2002.
[27] Hotelling H. Analysis of a complex of statistical variables into principal components. J Educ Psychol 1933;24(6):417–41.
[28] Brown CE. Applied multivariate statistics in geohydrology and related sciences. Berlin: Springer; 1998.
[29] Jolliffe IT. Principal component analysis. New York: Springer; 2002.
[30] Reilly TE, Plummer LN, Phillips PJ, Busenberg E. The use of simulation and multiple environmental tracers to quantify groundwater flow in a shallow aquifer. Water Resour Res 1994;30(2):421–33.
[31] Merkel BJ, Planer-Friedrich B. Groundwater geochemistry: a practical guide to modeling of natural and contaminated aquatic systems. Berlin: Springer; 2008.
[32] Batoit C, Emblanch C, Blavoux B, Simler R, Daniel M. Organic matter in karstic aquifers: A potential tracer in the carbon cycle. A small-scale laboratory model approach. IAHS Pub 2000;262:459–63.
[33] Wigley TML, Plummer LN. Mixing of carbonate waters. Geochim Cosmochim Acta 1976;40(9):989–95.
[34] Fitts CR. Groundwater science. San Diego: Elsevier Press; 2002.
[35] Whitaker FF, Smart PL. Groundwater circulation and geochemistry of a karstified bank-marginal fracture system, South Andros Island, Bahamas. J Hydrol 1997;197(1–4):293–315.
[36] Dong JJ, Tu CH, Lee WR, Jheng YJ. Effects of hydraulic conductivity/strength anisotropy on the stability of stratified, poorly cemented rock slopes. Comput Geotech 2012;40:147–59.
[37] Záruba Q, Mencl V. Engineering geology: developments in geotechnical engineering. New York: American Elsevier Publishing Company, Inc.; 1976.